International Journal of Biological Macromolecules 267 (2024) 131501

Contents lists available at ScienceDirect

International Journal of Biological Macromolecules

journal homepage: www.elsevier.com/locate/ijbiomac

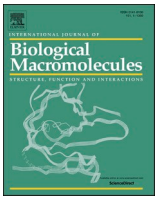

# Incorporating silver nanoparticles into electrospun nanofibers of casein/polyvinyl alcohol to develop scaffolds for tissue engineering

Nisha George [a], Sohini Chakraborty [b], N.L. Mary [b,*], L. Suguna [c]

[a] Department of Chemistry, St. Joseph's College (Autonomous), Irinjalakuda, Kerala, India
[b] Department of Chemistry, Stella Maris College (Autonomous), Chennai, Tamil Nadu, India
[c] Biotechnology and Biochemistry, CSIR- Central Leather Research Institute, Chennai, Tamil Nādu, India

ARTICLE INFO

*Keywords:*
Nanofibrous scaffold
Ag nanoparticles
Diabetic wound healing

ABSTRACT

Developing novel antimicrobial wound dressings that have the potential to address the challenges associated with chronic wounds is highly imperative in providing effective infection control and wound healing support. Biocompatible electrospun nanofibers with their high porosity and surface area enabling efficient drug loading and delivery have been investigated in this regard as viable candidates for chronic wound care. Here, we design Casein/Polyvinyl alcohol (CAN/PVA) nanofibers reinforced with silver nanoparticles (Ag NPs) by the electrospinning technique to develop diabetic wound healing scaffolds. The prepared samples were characterized using spectroscopic and electron microscopic techniques. The biocompatibility of the polymer samples were assessed using 3 T3 fibroblast cell lines and the maximum cell viability was found to 95 % at a concentration of 50 μg/mL for the prepared nanofibers. Scratch assay tests were also performed to analyze the wound healing activity of the nanofibers wherein they demonstrated increased migration and proliferation of fibroblast 3 T3 cells. Moreover, these nanofibers also exhibit antibacterial efficiency against Gram-negative bacteria, *Escherichia coli (E.coli)*. Therefore, the antimicrobial nature of the electrospun nanofibers coupled with their moisture absorption properties and wound healing ability render them as effective materials for wound dressing applications.

## 1. Introduction

Design and fabrication of functional biomaterials is essential to revolutionize research in the field of restorative biotherapeutics. [1–3] Due to the regenerative nature of the skin, wound healing can be deemed as a rational objective of regenerative medicine. Chronic non-healing wounds are one of the most common complications in diabetic patients and can be challenging to treat due to impaired wound healing processes. A hyperglycemic microenvironment results in delayed re-epithelialization, insufficient vascular lesions, and insufficient extracellular matrix (ECM) synthesis in diabetic wounds [4]. By eliminating oxidative stress, inflammation, and bacteria, one can effectively treat diabetic wounds [5,6].

Polymeric materials, both natural and synthetic have been used extensively in diabetic wound dressings owing to their physicochemical characteristics and biological activity. They provide numerous advantages, such as the ability to engineer tissue, dress wounds, and drug delivery. The production of nanofibers for skin regeneration has been reported previously using natural polymers such as collagen, Chitosan, and gelatin blended with synthetic polymers such as poly (−caprolactone) (PCL), poly(lactide-*co*-glycolide) (PLGA), and PVA [7]. These polymers showed accelerated hemostatic activity and wound healing due to their increased thrombin generation and stable blood clot formation. In recent studies, nanofibers have been shown to be structurally similar to native ECM and to promote skin regeneration [4]. Fibrous polymer matrices such as PVA produced by electrospinning have also been widely used for cell culture studies [8–9]. Due to its rubbery and elastic nature with high degree of swelling in water and biological fluids coupled with its high biodegradability and biocompatibility, PVA closely simulates biological tissue and is beneficial for wound dressing applications. Casein which is a natural milk protein that is a good source of bioactive peptides and serves as a very good antidiabetic agent has also been used in this respect to improve wound healing. The impact of nanotechnology in recent years has also led to the advancement in the field of bioengineering [10]. Novel materials can be synthesized by the appropriate selection of a biopolymer and nanofiller to affect specific applications [11,12]. Incorporation of biologically relevant nanoparticles can further improve the wound healing properties owing to

* Corresponding author.
*E-mail address:* maryterrysmc@gmail.com (N.L. Mary).

https://doi.org/10.1016/j.ijbiomac.2024.131501
Received 11 July 2023; Received in revised form 18 March 2024; Accepted 8 April 2024
Available online 16 April 2024

their excellent overall biological properties and high surface to volume ratio. Hybrid nanocomposites represent the combination of diverse functionalities of individual materials that exhibit good potential for therapeutic and diagnostic applications [13]. Bioimaging and disease treatment are important areas wherein these nanocomposites find utility. The applicability of these nanocomposites relies heavily on the filler-matrix interactions, filler type and concentration [14–17]. Nanoparticles and biologically active fragments that combine to form nanocomposites or nanofibers are optimal for drug delivery and wound healing applications [18–21]. It is possible to tailor electrospun nanofibers and load them with active agents in order to develop solutions for wound care that are effective. These applications are vital in the treatment of diabetic wounds which are generally more susceptible to infections [22]. High chemical inertness and SPR property of Ag NPs were employed for the preparation of hybrid nanocomposites [23]. Reports suggest that a green electrolysis of Ag-decorated $MoS_2$ nanocomposites and curcumin stabilized Ag NPs incorporated nanofibers shows an enhanced antibacterial effect and low cytotoxicity [24,25]. SBA-15/polydopamine (PDA)/Ag nanocomposites were used as an efficient nanocatalyst and microbial agent [26]. Also, Ag NPs, incorporated in polyvinyl alcohol melamine formaldehyde film, were used for wound dressing in diabetic patients [27]. Thus, the incorporation of different type of antidiabetic, anti-inflammatory and antibacterial therapeutic nanomaterials into nanofibers improve their efficacy as bioactive dressing with reduction of adverse side effects [28],

.Here, we report the fabrication of Casein/Polyvinyl Alcohol (CAN/PVA) films and nanofibers reinforced with Ag NPs. The nanofiber and films were functionalized by incorporating Ag NPs to formulate smart materials for enhanced nonlinear applications [29]. Moreover, the nanofiber scaffold can mimic the extracellular matrix, providing structural support to cells and facilitating tissue regeneration. Characterization was performed using Attenuated Total Reflectance-Fourier Transform Infrared (ATR-FTIR) spectroscopy, Ultraviolet-Visible (UV–Vis) Spectroscopy, Scanning Electron Microscopy (SEM), Transmission Electron Microscopy (TEM), Differential Scanning calorimetry (DSC) and X-Ray diffraction studies (XRD). The fabricated films and nanofibers demonstrated remarkable antibacterial activity upon contact with Gram-negative bacteria. In addition, an MTT assay using 3 T3 cell lines was performed to study the wound healing activity of the films. The results demonstrated that the nanofibers with incorporated Ag exhibited significantly greater scratch wound closure compared to the film. CAN/PVA nanofibrous mats have been used previously for wound dressing applications [30]. Similarly, PVA/hyaluronic acid/L-arginine nanofibers have also shown effectiveness in wound gap closure [31]. Casein glycerol-based wound dressing films have also been reported. [32] However, to the best of our knowledge, Ag NPs incorporated electrospun nanofibers of CAN/PVA have not been reported till date. The nanofibers prepared in the present work exhibit complete wound closure within 48 h. CAN was selected for dressing production due to its biocompatibility, biodegradability, stability, non-toxicity, and cost-effectiveness. Moreover, its antimicrobial and antihypertensive properties aid in diabetes prevention and control, thereby enhancing wound healing potential. PVA was employed to enhance the electrospinnability of CAN due to its biocompatibility, chemical resistance, and moisture absorption capabilities. Thus, the combination of these polymers enables wound dressing potential with optimal characteristics. Furthermore, the incorporation of Ag NPs augmented the dressing's antibacterial activity. Thus, based on the enhanced wound healing and antibacterial activity, these electrospun nanofibers have demonstrated excellent biocompatibility and cell growth promotion, presenting new avenues for chronic wound care in tissue engineering.

## 2. Materials and methods

### 2.1. Preparation of CAN/PVA film and nanocomposite film

For the present synthesis, CAN ($M_w$ = 2061) and PVA ($M_w$ = 140,000) were purchased from Aldrich Chemie. Silver nitrate ($AgNO_3$) and Sodium Hydroxide (NaOH) were purchased from Sigma Aldrich. All of the chemicals were used without further purification and Milli Q water was used as a solvent. Citrate capped Ag NPs were prepared by a method reported by us earlier [33]. The solutions of CAN and PVA were prepared by dissolving powdered chemicals to a concentration of 3 wt% in Milli Q water and stirred at room temperature for 30 min. The blending process of CAN/PVA at 30:70 weight ratio was carried out using a probe sonicator. The synthesized Ag NPs were added at a concentration of 0.15 wt% relative to the total weight of the polymer blend. The dispersion process was carried out by sonication for 30 min to ensure an even distribution of the NPs throughout the polymer matrix. Solution casting method was used to prepare both CAN/PVA films and its Ag nanocomposites (CAN/PVA-S1). In this method, the polymer blend and the nanocomposite solution were cast into the Petri dish and allowed to dry to obtain CAN/PVA and CAN/PVA-S1 films.

### 2.2. Preparation of composite nanofibers

Electrospinning was used for the preparation of nanofibers. In a 5 mL syringe, the Ag NPs reinforced CAN/PVA solution as prepared above was loaded. A DC voltage of 20–25 kV was applied between the syringe and collector which was covered with Aluminium foil and a flow rate of 0.6 mL/h was maintained. As the jet moved towards the collector, the solvent evaporated and composite nanofibers (CAN/PVA-S2) were formed and deposited on the Aluminium foil.

### 2.3. Antibacterial activity: well/disk diffusion method

Agar well/disc diffusion method was used to study the antibacterial activity of the nanocomposites [34,35]. Bacterial culture of *Escherchia-coli (E. coli)* was swabbed on freshly prepared nutrient agar which was poured on sterile petridishes. After solidification, the prepared polymer samples at different concentrations (25, 50, 75, 100 μg/mL) were loaded in wells/discs and the plates were incubated at 37 °C for 24 h. An inhibitory zone was measured in mm around each well/disc after incubation.

### 2.4. Cell viability determination by MTT assay

MTT (3-(4,5-dimethylthiazol-2-yl)-2,5-diphenyltetrazolium bromide) assay is a quantitative colorimetric method for the determination of cell survival and proliferation [22]. The assessed parameter is the metabolic activity of viable cells. 3 T3 mouse fibroblast cells were seeded in a 96-well plate at a density of $1 \times 10^5$ cells. The cells were incubated overnight at 37 °C and 5 % $CO_2$ with a complete medium. After 70 % confluence, the complete medium was replaced with an incomplete medium containing different concentrations of working solution of prepared nanocomposites (25, 50, 75 and 100 μg/mL) for 24 h and 48 h. At the end of the incubation period, the medium was discarded and replaced with fresh incomplete medium containing 10 μL of MTT and incubated for 4 h at 37 °C and 5 % $CO_2$. The MTT containing medium was then discarded and 100 μL of sterile DMSO was added to each well to dissolve the obtained purple formazan crystals. The amount of formazan crystals formed is indicative of the mitochondrial oxidation of MTT and the plate was read at 595 nm.

$$\text{Percentage of cell viability} = (A_{595}\text{nmoftreatedcells}/A_{595}\,\text{nm of control}) \times 100.$$

### 2.5. In vitro wound healing assay (Scratch assay)

The *in vitro* wound healing assay was performed by the method described by Liang et al. 2007 [36]. The direct contact method was used in the scratch assay. 3 T3 mouse fibroblast cells were seeded in 6 well tissue culture dishes ($1 \times 10^5$ cells/well). After the confluence was reached, cell monolayers were incubated in serum free medium for 12 h. After 12 h, the cell monolayers were gently scratched with a sterile pipette tip to create the wound and extensively rinsed with medium to remove all cellular debris. 100 μL of the nanocomposites were added and incubated for 24 h and 48 h. The rate of cell migration and healing was assessed by placing the cells under an inverted microscope and photographing them. Subsequently, the cells' ability to migrate and fill the gap over time was monitored. Manual image analysis was then employed to measure the remaining wound area. The scratch healing rate was analyzed as the decrease in wound area over time, normalized by the initial wound area.

## 3. Results and discussion

### 3.1. ATR-FTIR absorption spectra

FTIR spectroscopy was used to identify the functional groups involved in polymer blends as well as their unique interaction with nanoparticles. The recorded FT-IR spectra of the polymer blend and its nanocomposites are presented in Fig. 1. The stretching and bending vibrations of the hydrogen bonding –OH group of CAN/PVA blend was observed at 3040–3650 $cm^{-1}$ and 1630–1650 $cm^{-1}$ [37]. A strong absorption band at 2927 $cm^{-1}$ corresponds to the -C-H stretching frequency. The characteristic peaks of CAN are observed at 1639, 1534, 1442 and 1229 $cm^{-1}$ which corresponds to -C=O stretching, both -C-N stretching and -N-H bending, -C-H deformation and -N-H deformation, respectively [38]. The absorption bands at 1080 and 915 $cm^{-1}$ indicate stretching and bending vibrations of -C-O groups in PVA [28]. The -C═O stretching frequency shifts from 1635 $cm^{-1}$ in CAN/PVA to 1639 $cm^{-1}$ in CAN/PVA-S1. Similar observations were reported in the case of nanocomposites of PVP with Ag NPs [39]. The IR spectra of CAN/PVA-S2 was found to be essentially the same as the solvent casted films of CAN/PVA-S1. Analogous findings were also reported in the case of PEO and Nylon 6 nanofibers and films [40,41]. Therefore, it may be concluded that there are no structural changes in the polymer samples during the fabrication of nanofibers.

### 3.2. UV–Visible absorption spectroscopy

UV–Visible absorption spectroscopy was performed for CAN/PVA, CAN/PVA-S1 and CAN/PVA-S2 in water and the spectra are given in Fig. 1(d). These spectra indicate that the SPR peak is observed at 408 nm in the spectrum of CAN/PVA-S1 while the SPR phenomenon is indicated by the peak at 414 nm in the case of CAN/PVA-S2. These observations suggest that Ag NPs have been successfully incorporated into the polymer matrix of both the film and the nanofibers. These absorption bands match the characteristic SPR band of Ag NPs [42–43].

### 3.3. SEM analysis

Scanning Electron Microscopy (SEM) was used to study the morphology of the polymer blend CAN/PVA and the nanocomposites with metal NPs. The SEM images of the polymer samples are given in Fig. 2. The SEM image of CAN/PVA shows a continuous homogenous morphology which confirms the miscibility of the two polymers. The miscibility of the two polymers in the blend can be attributed to intermolecular hydrogen bonding between PVA and CAN. SEM micrograph of CAN/PVA-S1 shows the presence of Ag NPs in the matrix of the blend.

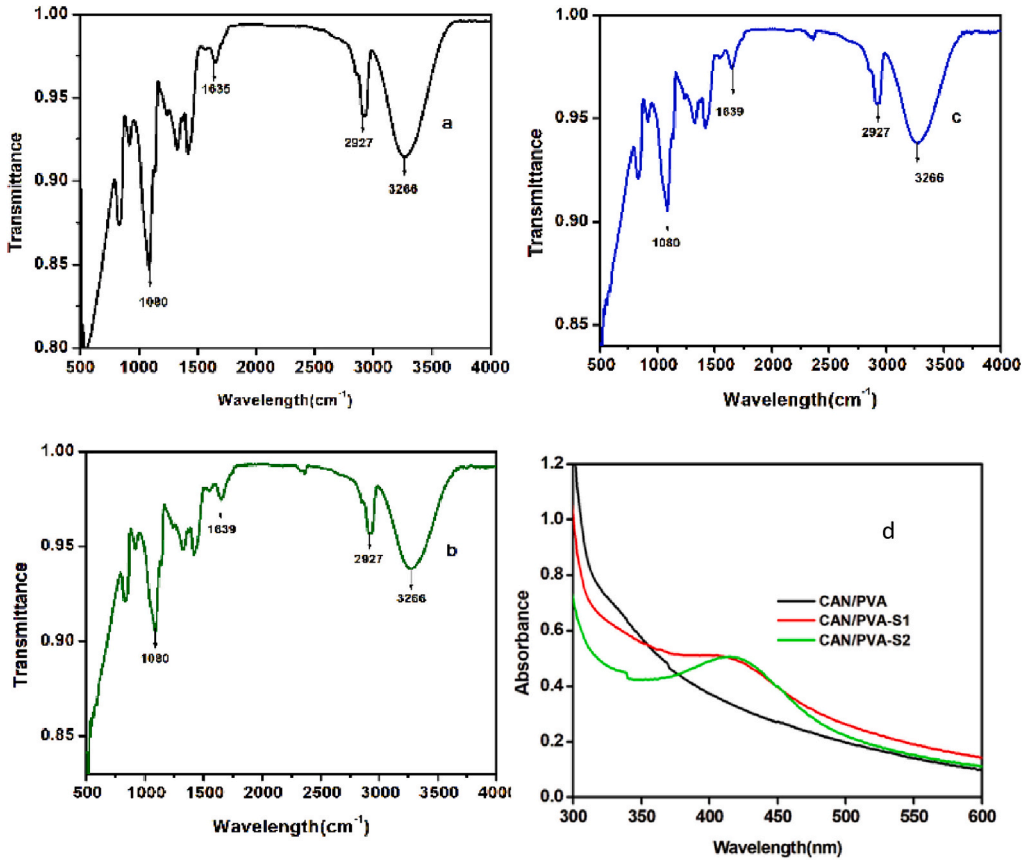


**Fig. 1.** ATR-FTIR spectrum of a) CAN/PVA b) CAN/PVA-S1 c) CAN/PVA-S2 d) UV–Visible absorption spectra of CAN/PVA, CAN/PVA-S1 and CAN/PVA-S2.

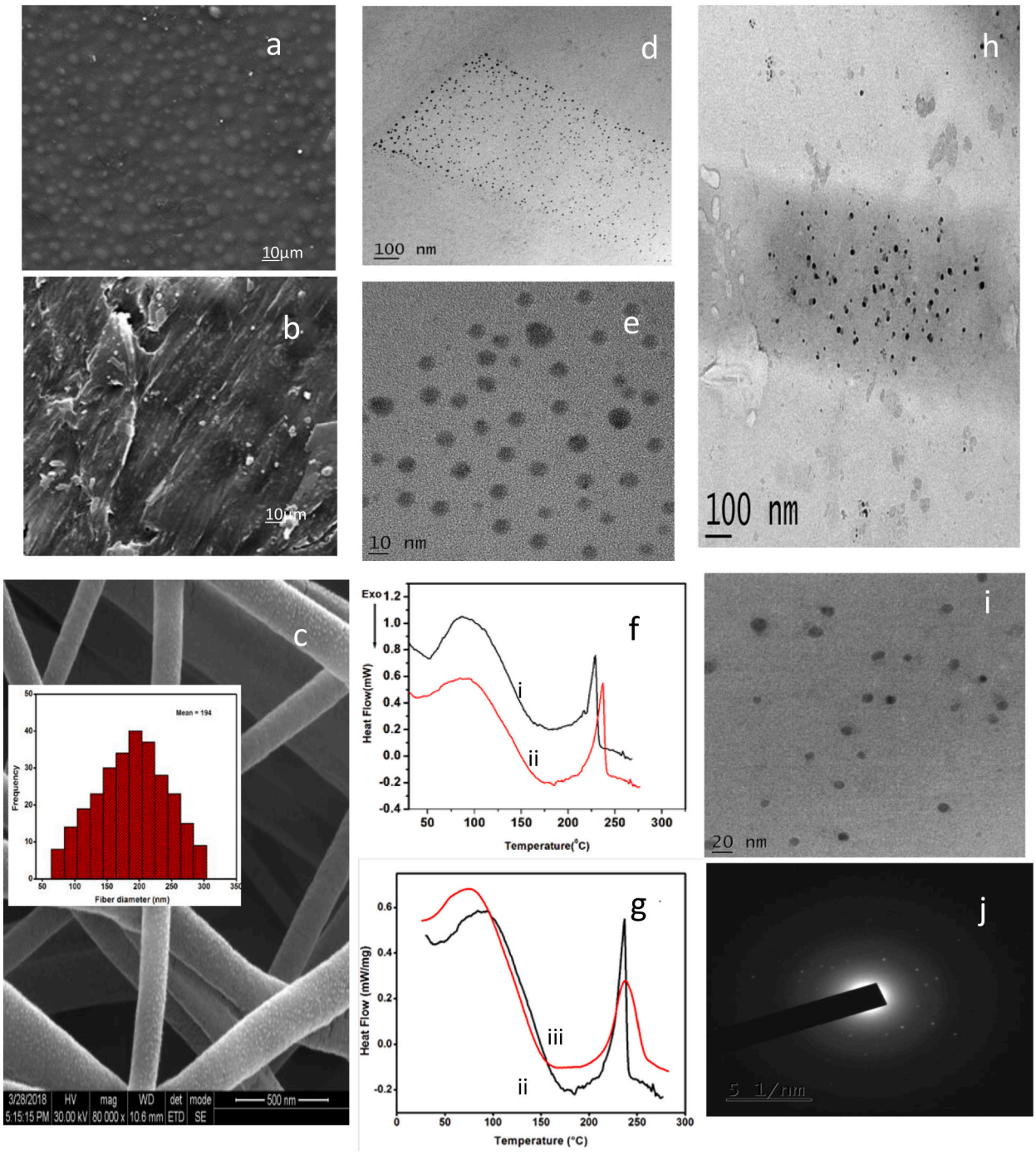


**Fig. 2.** SEM images of (a) CAN/PVA (600×), (b) CAN/PVA-S1(3000 X) c) SEM image and particle size distribution of CAN/PVA-S2 (80,000×) . TEM images of CAN/PVA-S1 at (d) lower and (e) higher magnification. TEM images h) lower magnification i) higher magnification and j) SAED pattern of CAN/PVA-S2. DSC thermograms of h) [i] CAN/PVA and [ii] CAN/PVA-S1. Comparative study of DSC thermograms g) of [i] CAN/PVA-S1 and [iii] CAN/PVA-S2 miscibility of the component polymers in the blend at this composition. Furthermore, the nanocomposites with metal NPs have higher Tm values than the CAN/PVA polymer blend. Thus, the introduction of Ag NPs in CAN/PVA blend enhanced the Tm value. Similar trend was also observed in case of the nanofibers as represented in Fig. 2(g), but here we observe a decrease in the Tg value due to the amorphous nature of nanofibers.

From the surface of the CAN/PVA films, it can be deduced that the PVA content has an influence on the physical characteristic of the blended film. A similar type of morphological change was reported earlier in the case of PVA/PAN blended film [44]. Basavarajeshwari et al. reported that a miscible blend was formed by the physical interaction of PVA and PVP [45]. SEM analysis was also carried out on CAN/PVA-S2 and Fig. 2 (c) shows the SEM images and size distribution of the nanofibers. The arrangements of nanofibers were fairly random with no distinct alignment in this case. However, the surface of the composite nanofibers are smooth, indicating good incorporation of Ag NPs into the CAN/PVA polymer blend.

### 3.4. TEM analysis

In order to determine the size of NPs in the nanocomposites of CAN/PVA, TEM investigation was carried out on the nanocomposites, namely,

CAN/PVA-S1. From the TEM analysis of CAN/PVA-S1 Fig. 2(d,e), effective incorporation of Ag NPs in the CAN/PVA matrix was re-affirmed. The average size of the NPs was found to be 8 nm. High Resolution Transmission Electron Microscopy (HR-TEM) and Selected Area Electron Diffraction Pattern (SAED) analyses were carried out on the electrospun nanofiber CAN/PVA-S2 and the images are given in Fig. 2(h, i,j). Along with the successful incorporation of Ag NPs incorporated in the CAN/PVA matrix, the SAED pattern also indicated the spherical shape of the NPs.

### 3.5. DSC analysis

The thermal transition behaviour of the polymer blend and its nanocomposites were determined using DSC analysis. DSC thermograms of the samples are given in Fig. 2(f,g) which provide insights into the glass transition temperature (Tg) and melting temperature (Tm). There are two endothermic peaks in each of the thermograms. The first peak corresponds to Tg and the second peak represents the Tm. On comparison of the DSC curve of CAN/PVA blend and its nanocomposites, it was found that the second endothermic peak (Tm) of the blend shifted to higher temperatures. It confirms the presence of Ag NPs in the blends and its enhanced thermal stability with the formation of different crystalline forms. Tg and Tm of the blend and Ag nanocomposites are tabulated in Table 1

Tg of CAN/PVA blend is found to be 84 °C which is in between the Tg of casein at 76 °C and that of pure PVA at 88 °C. This suggests that the polymers are miscible and compatible at this composition as is also observed from the TEM images. The nanocomposites containing Ag NPs have slightly higher Tg values than that of the blend. This indicates that the incorporation of Ag NPs increases the Tg value of the blend. Similarly, the melting temperature of CAN/PVA (231 °C) is in between the $T_m$ values of pure PVA (241 °C) and pure CAN (210 °C) indicating.

### 3.6. XRD analysis

The physical and mechanical properties of polymers and their nanocomposites are strongly dependent on the percentage and nature of their crystalline and amorphous regions. Also, this amount is responsible for chemical reactions, the absorptivity of dyes and pigments, and humidity in the case of polymeric fabrics. The reactivity will be higher when the amorphous part of the polymer is larger [46]. XRD has been used to characterise changes in the crystal structure parameters, including the degree of crystal orientation, the apparent crystal size, and the lattice strain along the axis of the crystal unit cell [47]. XRD diffraction patterns were obtained for three samples, namely, CAN/PVA, CAN/PVA-S1,CAN/PVA-S2 and the diffractograms are presented in Fig. 3. It may be seen in the diffraction pattern of CAN/PVA that there is a major peak at about $2\theta = 20^0$ which corresponds to the plane of pure PVA [48]. Since all the three samples contain PVA as the major component this is the main peak in diffraction patterns of the three samples. In the diffraction pattern of CAN/PVA, there is additional peak at a lower 2θ value (around $12^0$) and this peak is due to casein. A sharp and high intensity peak is seen at $2\theta = 5^0$ in the XRD pattern of CAN/PVA-S1 and also a sharp high intensity peak at about the same 2θ value in the case of CAN/PVA-S2. These observations establish that the two nanocomposites contain the metal NPs.

**Table 1**
Glass transition temperature (Tg), Melting temperature (Tm) of CAN/PVA and CAN/PVA-S1.

| Sample Name | Tg $^0$C | Tm $^0$C |
|---|---|---|
| CAN/PVA | 84 | 231 |
| CAN/PVA-S1 | 86 | 239 |

### 3.7. Antibacterial analysis of CAN/PVA-S2

The antibacterial efficacy of the nanofiber, CAN/PVA-S2 against gram negative bacteria- *Escherchia-coli (E.Coli)* was evaluated. Different concentration of the samples were tested and the results are shown in Fig. 4 (a) and Table 2. At a low concentration of 25 μg/mL, the zone of inhibition is found to be almost comparable to that of the control indicating enhanced antibacterial activity of the nanofibers. With the increase in concentration of the nanofiber, the zone of inhibition increases gradually signifying moderately effective antibacterial action even at higher concentrations. Casein is milk protein and is used for the antidiabetic and antibacterial study [49]. PVA has been used in various applications in the field of medicine, pharmaceuticals, *etc.* and Ag NPs has been reported to be non-toxic to human cells but shows toxicity to bacteria because of its affinity to proteins and nucleic acid [50].Additionally, the higher surface area to volume ratio of naofibers promotes greater antibacterial activity. Thus the increased antibacterial efficacy is due to the combined effect of all the three components comprising the nanofiber.

### 3.8. In vitro wound healing potential of CAN/PVA-S1 and CAN/PVA-S2 in 3 T3 fibroblast cell lines

Natural polymers such as collagen, Chitosan, and gelatin were blended with synthetic polymers of poly (ε-caprolactone) (PCL), poly (lactide-*co*-glycolide) (PLGA), PVA for the production of nanofibers for skin regeneration [51]. Recent studies have shown that nanofibers can offer a structural resemblance with native ECM and promote skin regeneration [52]. Due to its rubbery and elastic nature with high degree of swelling in water and biological fluids PVA closely simulates biological tissue and is beneficial for wound dressing applications. Excellent biological properties and the surface to volume ratio of Ag incorporated nanofibers make it a good material for wound healing [53].

The cell viability at different concentrations of CAN/PVA,CAN/PVA-S1 and CAN/PVA-S2 at 24 & 48 h of incubation are shown in Fig. 4 (b,c, d). For *in vitro* cell viability tests, both the film and nanofiber samples demonstrated a maximum cell viability of 95 % at a concentration of 50 μg/mL indicating the enhanced biocompatibility of these materials and their non-toxicity.

The proliferation and migration of 3 T3 cells were studied by using an *in vitro* wound healing assay in confluent culture. Cell proliferation is an essential event during re-epithelization, so proliferating fibroblast at the wound site ensures an adequate supply of cells to migrate and cover the wound surface. Synthesis of an extracellular matrix (ECM) is a key feature of wound healing. Dermal reconstruction is characterized by the formation of granulation tissue, which includes cell proliferation, ECM deposition, wound contraction and angiogenesis. Scratch assay using 3 T3 cell lines was performed to study the wound healing activity of films and nanofibers as shown in Fig. 4 (e-m). The migration rate of 3 T3 cells was evaluated until complete healing. After making scratch wounds, the cells were supplemented with 50 μg/mL of sample and photomicrographs were taken using inverted microscope to assess the healing activity at different time intervals. Based on the *in vitro* scratch wound assay, CAN/PVA-S2 showed increased migration and proliferation of fibroblast 3 T3 cells. Migration and proliferation of 3 T3 cells was also observed to confirm the therapeutic activity of CAN/PVA-S2 in wound healing. The images indicated efficient migration and proliferation of the fibroblast cells and hence the sample served as a good material to enhance the *in vitro* wound healing ability. From the results, it can be depicted that the nanofibers with incorporated Ag shows complete closure of the wound when compared to the film. This can be attributed to the fact that electrospun nanofibers require shorter response time and excise more control over the release rate of the drug thereby resulting in efficient wound healing [54]. Additionally, the use of nanofiber scaffolds can be beneficial in diabetic wound treatment due to their ability to promote wound healing and prevent infection. The small size of the

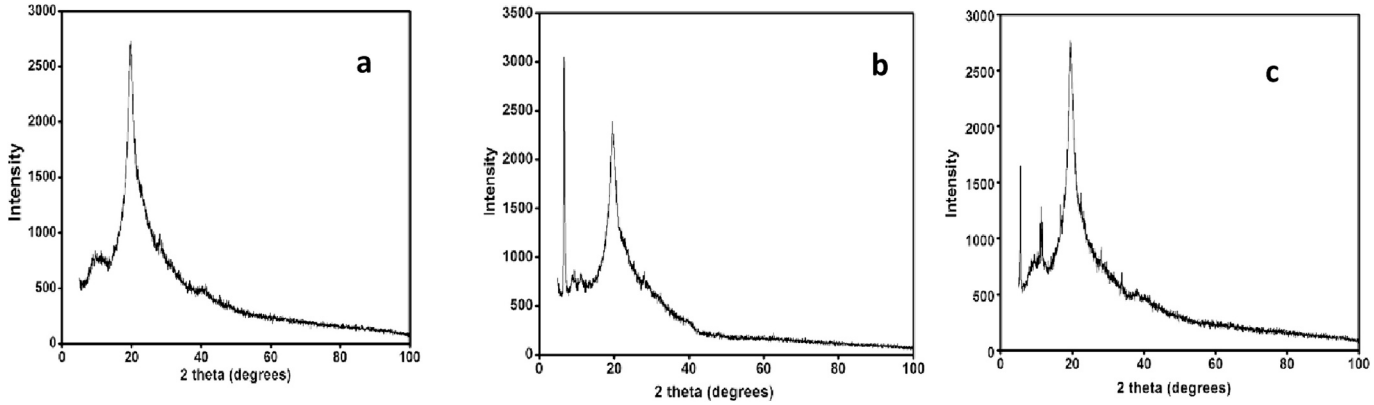


**Fig. 3.** XRD patterns for (a) CAN/PVA, (b) CAN/PVA-S1 (c) CAN/PVA-S2.

***In vitro* wound healing potential of CAN/PVA-S1 and CAN/PVA-S2 in 3T3 fibroblast cell lines**

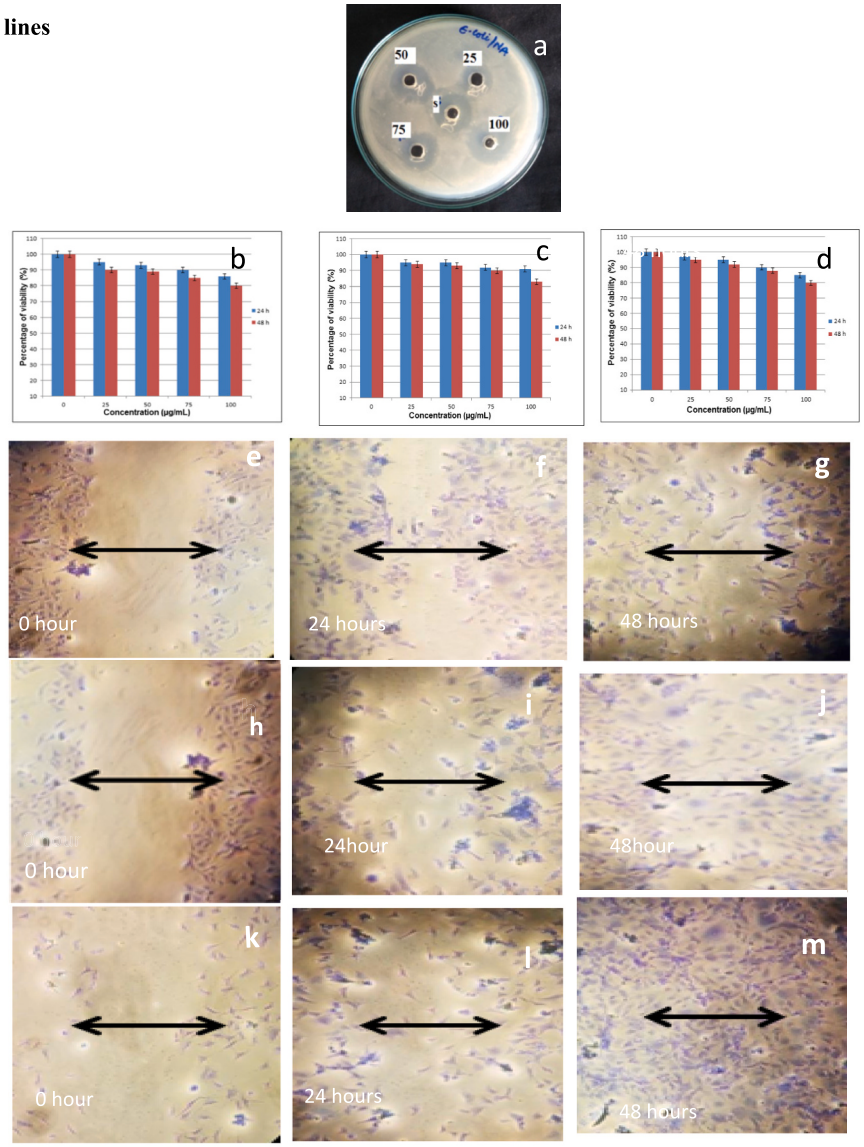


**Fig. 4.** a) Effect of different concentrations of CAN/PVA-S2 on the zone of inhibition. Percentage of cell viability of 3 T3 cells in b) CAN/PVA c) CAN/PVA-S1 d) CAN/PVA-S2. *In vitro* wound healing of 3 T3 cells treated with CAN/PVA at e) 0 h f) 24 h g) 48 h *In vitro* wound healing of 3 T3 cells treated with CAN/PVA-S1 at h) 0 h i) 24 h j) 48 h. *In vitro* wound healing of 3 T3 cells treated with CAN/PVA-S2 at k) 0 h l) 24 h m) 48 h.

**Table 2**
Results obtained using 4 different concentrations of the nanofiber, CAN/PVA-S2 by *E. coli* culture.

| Concentration (μg/mL) | Zone of inhibition (mm) |
|---|---|
| 25 | 13 |
| 50 | 15 |
| 75 | 16 |
| 100 | 18 |
| Control | 14 |

nanofibers provides a large surface area, which can support cell adhesion proliferation and migration aiding in the wound closure process.

## 4. Conclusion

In conclusion, in this study, we have successfully fabricated CAN/PVA film and its nanocomposites functionalized with Ag NPs by solution casting method. Additionally, electrospinning technique was employed to prepare composite nanofibers. Spectral and morphological studies confirmed the formation of composite films and nanofibers. The appearance of characteristic absorption peaks in the UV–Vis spectrum at specific wavelengths indicated the presence of Ag NPs, confirming the successful functionalization of the polymer blend. DSC analysis reveals that the polymer blend is miscible and compatible at the studied composition, and the incorporation of metal nanoparticles enhances both the Tg and Tm values of the blend and its nanocomposites. The nanofiber also exhibits a similar trend but with a decrease in Tg value due to their amorphous nature. Both the film and the nanofiber show a maximum cell viability of 95 % at 50 μg/mL against mouse fibroblast cells. MTT tests showed greater scratch wound closure for Ag incorporated nanofibers when compared to the films. Considering these findings, the nanofiber scaffold developed through electrospinning, particularly Ag NPs incorporated nanofibers holds promise for treating diabetic wounds and preventing infection. The nanofiber scaffold could potentially serve as a supportive frame work or scaffold for the growth of the cells and facilitate the healing process in diabetic wounds. Additionally, the presence of Ag NPs within the nanofibers could contribute to the prevention of bacterial infections, which are commonly associated with diabetic wounds.

## CRediT authorship contribution statement

**Nisha George:** Writing – review & editing, Writing – original draft, Software, Methodology, Conceptualization. **Sohini Chakraborty:** Writing – review & editing. **N.L. Mary:** Writing – review & editing, Methodology, Conceptualization. **L. Suguna:** Writing – review & editing.

## Declaration of competing interest

We wish to confirm that there are no known conflicts of interest associated with this publication and there has been no significant financial support for this work that could have influenced its outcome.

## Data availability

No data was used for the research described in the article.

## Acknowledgments

The author Nisha George acknowledge DST-FIST (SR/FST/College-001/2009) and KSCSTE-SARD (KSCSTE/623/2019-SARD) for providing the instrumental facilities.

## Appendix A. Supplementary data

Supplementary data to this article can be found online at https://doi.org/10.1016/j.ijbiomac.2024.131501.

## References

[1] S.A. Eming, P., M. Martin, Tomic-Canic, wound repair and regeneration: mechanisms, signaling, and translation, Sci. Transl. Med. 6 (265) (2014) 1946–6242.
[2] N. Pazyar, R. Yaghoobi, et al., Skin wound healing and phytomedicine: a review, Skin Pharmacol. Physiol. 27 (2014) 303–310.
[3] R. Krishnan, R., R. Rajeswari, et al., Polysaccharide nanofibrous scaffolds as a model for in vitro skin tissue regeneration, J. Mater. Sci. Mater. Med. 23 (2012) 1511–1519.
[4] X. Wang, B. Ding, B. Li, Biomimetic electrospun Nanofibrous structures for tissue engineering, Mater. Today 16 (6) (2013) 229–241.
[5] W.E. Teo, W., S. Ramakrishna, A review on electrospinning design and nanofibre assemblies, Nanotechnology 17 (2006) 89–106.
[6] J. Li, et al., 3D printing of hydrogels: rational design strategies and emerging biomedical applications, Mater. Sci. Eng. R 140 (2020) 100543.
[7] D. Bhattarai, L. Aguilar, C. Park, C. Kim, A Review on Properties of Natural and Synthetic Based Electrospun Fibrous Materials for Bone Tissue Engineering, Membranes (Basel) 8 (3) (2018) 62.
[8] F. Yoshii, Y., K. Zhanshan, K. Isobe, K. Shinozaki, Electron beam crosslinked PEO and PEO/PVA hydrogels for wound dressing, Radiat. Phys. Chem. 55 (2) (1999) 133–138.
[9] F. el Mohtadi, R., X. D'Arcy, Z. Yang, Y. Turhan, A., N. Alshamsan, Main chain polysulfoxides as active 'stealth' polymers with additional antioxidant and anti-inflammatory behaviour, Int. J. Mol. Sci. 20 (2019) 18.
[10] S. Phadtare, S. Shah, A. Prabhune, P.P. Wadgaonkar, M. Sastry, Immobilization of Candida Bombicola cells on free-standing organic-gold nanoparticle membranes and their use as enzyme sources in biotransformations, Biotechnol. Prog. 20 (6) (2004) 1817–1824.
[11] D. Kossyvaki, G. Suarato, M. Summa, A. Gennari, N. Francini, I. Gounaki, et al., Keratin–cinnamon essential oil biocomposite fibrous patches for skin burn care, Mater. Adv. 1 (6) (2020) 1805–1816.
[12] M. Beck-Broichsitter, M. Thieme, J. Nguyen, T. Schmehl, T. Gessler, W. Seeger, et al., Novel "Nano in Nano" composites for sustained drug delivery: biodegradable nanoparticles encapsulated into nanofiber non-wovens, Macromol. Biosci. 10 (12) (2010) 1527–1535.
[13] Z. Wei, M. Wang, et al., Sodium alginate as an eco-friendly rheology modifier and salt-tolerant fluid loss additive in water-based drilling fluids, RSC Adv. 12 (2022) 29677–29687.
[14] A. Kumar, S. Huo, X. Zhang, J. Liu, A. Tan, S. Li, S. Jin, X. Xue, Y. Zhao, T. Ji, et al., Neuropilin-1-targeted gold nanoparticles enhance therapeutic efficacy of platinum (IV) drug for prostate cancer treatment, ACS Nano 8 (5) (2014) 4205–4220.
[15] X. Wang, S. Li, P. Zhang, F. Lv, L. Liu, L. Li, S. Wang, An optical nanoruler based on a conjugated polymer-silver nanoprism pair for label-free protein detection, Adv. Mater. 27 (39) (2015) 6040–6045.
[16] J. Lazarovits, Y.Y. Chen, E.A. Sykes, W.C.W. Chan, Nanoparticle-blood interactions: the implications on solid tumour targeting, Chem. Commun. 51 (14) (2015) 2756–2767.
[17] T.L. Doane, C. Burda, The unique role of nanoparticles in nanomedicine: imaging, drug delivery and therapy, Chem. Soc. Rev. 41 (7) (2012) 2885–2911.
[18] Q. Shi, N. Vitchuli, J. Nowak, J.M. Caldwell, F. Breidt, M. Bourham, X. Zhang, M. McCord, Durable antibacterial Ag/polyacrylonitrile (Ag/PAN) hybrid nanofibers prepared by atmospheric plasma treatment and electrospinning, Eur. Polym. J. 47 (7) (2011), 1402–140.
[19] L. Zhou, L. Cai, H. Ruan, et al., Electrospun chitosan oligosaccharide/polycaprolactone nanofibers loaded with wound-healing compounds of Rutin and Quercetin as antibacterial dressings, Int. J. Biol. Macromol. 183 (2021) 1145–1154.
[20] Li Zhang, J. Yang, X. Zhu, et al., Electrospun nanofibrous membranes loaded with IR780 conjugated MoS2-nanosheet for dual-mode photodynamic/photothermal inactivation of drug-resistant bacteria, Environ. Technol. Innov. 30 (2023) 103098.
[21] Dual-drug delivery of Ag-chitosan nanoparticles and phenytoin via core-shell PVA/PCL electrospun nanofibers, Carbohydr. Polym. 270 (2021) 118373.
[22] T. Hirsch, M. Spielmann, B. Zuhaili, T. Koehler, M. Fossum, H.U. Steinau, F. Yao, L. Steinstraesser, A.B. Onderdonk, E. Eriksson, Enhanced susceptibility to infections in a diabetic wound healing model, BMC Surg. 8 (2008) 1–8.
[23] N. George, R. Subha, A. Rose, N.L. Mary, Plasmon enhanced two-photon absorption in modified styrene – maleic anhydride silver nanocomposites, Nano-Structures & Nano-Objects 11 (2017) 32–38.
[24] Qilan Xu, Yuhui Liu, Ling Cai, et al., A green electrolysis of silver-decorated $MoS_2$ nanocomposite with an enhanced antibacterial effect and low cytotoxicity, Nanoscale Adv. 3 (2021) 3460.
[25] L. Cai, X. Zhu, H. Ruan, J. Yang, Curcumin-stabilized silver nanoparticles encapsulated in biocompatible electrospun nanofibrous scaffold for sustained eradication of drug-resistant bacteria, J. Hazard. Mater. 452 (2023) 131290.
[26] Y. Song, H. Jiang, B. Wang, Y. Kong, J. Chen, Silver-incorporated mussel-inspired polydopamine coatings on mesoporous silica as an efficient nanocatalyst and antimicrobial agent, ACS Appl. Mater. Interfaces 10 (2) (2018) 1792–1801.

[27] Kakkar, K. Madgula, Y.V.S. Nehru, J. Kakkar, Polyvinyl alcohol - melamine formaldehyde films and coatings with silver nano particles as wound dressings in diabetic foot disease, Eur. Chem. Bull. 4 (2) (2015) 98–105.
[28] L. Cai, Y. Haung, Y. Daun, et al., Schiff-base silver nanocomplexes formation on natural biopolymer coated mesoporous silica contributed to the improved curative effect on infectious microbes, Nano Res. 14 (8) (2021) 2735–2748.
[29] N. George, R. Subha, A. Rose, N.L. Mary, Plasmon enhanced two-photon absorption in modified styrene – maleic anhydride silver nanocomposites, Nano-Structures & Nano-Objects 11 (2017) 32–38.
[30] S. Biranje, P. Madiwale, R.V. Adivarekar, Porous electrospun casein/PVA nanofibrous mat for its potential application as wound dressing material, J.Porous Mater. 26 (2019) 29–40.
[31] Y. Hussein, et al., Electrospun PVA/hyaluronic acid/L-arginine nanofibers for wound healing applications: nanofibers optimization and in vitro bio evaluation, Int.J. Biol.Macromol 164 (2020) 667–676.
[32] D. Kolahreez, et al., Multifunctional casein-based wound dressing capable of monitoring and moderating the proteolytic activity of chronic wounds, Biomacromolecules 25 (2024) 700–714.
[33] W.E. Teo, S. Ramakrishna, A review on electrospinning design and nanofibre assemblies, Nanotechnology 17 (2006) 89–106.
[34] J. Li, et al., 3D printing of hydrogels: rational design strategies and emerging biomedical applications, Mater. Sci. Eng. R 140 (2020) 100543.
[35] C. Liang, A.Y. Park, J. Guan, In vitro scratch assay: a convenient and inexpensive method for analysis of cell migration in vitro, Nat. Protoc. 2 (2) (2007) 329–333.
[36] S. Burikov, T. Dolenko, S. Patsaeva, Y. Starokurov, Raman and IR spectroscopy research on hydrogen bonding in water – ethanol systems, Mol. Phys. 108 (18) (2010) 2427–2436.
[37] R.N. Oliveira, M.C. Mancini, F. Cabral, S. De Oliveira, T.M. Passos, B. Quilty, FTIR analysis and quantification of phenols and flavonoids of five commercially available plants extracts used in wound healing, Rev. Matéria 21 (3) (2016) 767–779.
[38] E.E. Tănase, M.E. Popa, M. Râpă, O. Popa, Preparation and characterization of biopolymer blends based on polyvinyl alcohol and starch, Rom. Biotechnol. Lett. 20 (2) (2015) 10306–10315.
[39] M. Wang, Y. Song, M. Wang, X. Zhang, J. Wu, T. Zhang, Investigation on the role of the molecular weight of polyvinyl pyrrolidone in the shape control of high-yield silver nanospheres and nanowires, Nanoscale Res. Lett. 9 (17) (2014) 1–8.
[40] M. Krstić, M. Radojević, D. Stojanović, V. Radojević, P. Uskoković, S. Ibrić, Formulation and characterization of nanofibers and films with carvedilol prepared by electrospinning and solution casting method, Eur. J. Pharm. Sci. 101 (2017) 160–166.
[41] E. Fatarella, D. Spinelli, M. Ruzzante, R. Pogni, Nylon 6 film and nanofiber carriers: preparation and laccase immobilization performance, J. Mol. Catal. B: Enzym. 102 (2014) 41–47.
[42] W. Haiss, N.T.K. Thanh, J. Aveyard, D.G. Fernig, Determination of size and concentration of gold nanoparticles from UV - vis spectra, Anal. Chem. 79 (11) (2007) 4215–4221.
[43] C. Ramteke, T. Chakrabarti, B.K. Sarangi, R. Pandey, Synthesis of silver nanoparticles from the aqueous extract of leaves of Ocimum Sanctum for enhanced antibacterial activity, J. Chem. 2013 (2013) 1–7.
[44] G. Zhu, F. Wang, K. Xu, Q. Gao, Y. Liu, Study on properties of poly ( vinyl alcohol )/ polyacrylonitrile blend film ARTIGO CIENTÍFICO, Polímeros Ciência e Tecnol. 23 (2013) 146–151.
[45] B.M. Baraker, B. Lobo, Experimental study of PVA-PVP blend films doped with cadmium chloride monohydrate, Indian J. Pure Appl. Phys. 54 (10) (2016) 634–640.
[46] Y.W.E. Matsubara, K. Shinoda, X-Ray Diffraction Crystallography Introduction, Examples and Solved Problems, Springer, Heidelberg Dordrecht London New York, 2011.
[47] Z. Ullah, S. Atiq, S. Naseem, Indexing the diffraction patterns and investigating the crystal structure of Pb-doped strontium ferrites, J. Sci. Res. 5 (2) (2013) 235–244.
[48] W. Brockmann, J. K.-K, Polypropylene: An A-Z Reference, Springer, Netherlands, 1999.
[49] A. Usman, Z. Hussain, S. Sim Riaz, Enhanced nonlinear optical properties of reduced graphene oxide decorated with silver nanoparticles, Carbohydr. Polym. 8 (3) (2018) 836–841.
[50] X. Wang, B. Ding, B. Li, Biomimetic electrospun nanofibrous structure s for tissue engineering, Mater. Today 16 (6) (2013) 229–241.
[51] D. Bhattarai, L. Aguilar, C. Park, C. Kim, A Review on Properties of Natural and Synthetic Based Electrospun Fibrous Materials for Bone Tissue Engineering, Membranes (Basel) 8 (3) (2018) 62.
[52] MI, E. S.; S, A, In vivo anti-diabetic and biological activities of milk protein and milk protein hydrolyaste, Adv. Dairy Res. 4 (2) (2016) 1–6.
[53] S. Zhang, Y. Tang, B. Vlahovic, A review on preparation and applications of silver-containing nanofibers, Nanoscale Res. Lett. 11 (1) (2016) 1–8.
[54] S. Chen, B. Liu, M.A. Carlson, A.F. Gombart, D.A. Reilly, J. Xie, Recent advances in electrospun nanofibers for wound healing, Nanomedicine 12 (11) (2017) 133.